Journal of Power Sources 264 (2014) 155–160

Contents lists available at ScienceDirect

Journal of Power Sources

journal homepage: www.elsevier.com/locate/jpowsour

Cathodes with intrinsic redox overcharge protection: A new strategy towards safer Li-ion batteries

Jian-Wu Wen [a,b], Da-Wei Zhang [a], Chun-Hua Chen [a,*], Chu-Xiong Ding [a], Yan Yu [a,c,**], Joachim Maier [c]

[a] CAS Key Laboratory of Materials for Energy Conversion, Department of Materials Science and Engineering & Collaborative Innovation Center of Suzhou Nano Science and Technology, University of Science and Technology of China, Anhui, Hefei 230026, China
[b] State Key Laboratory Cultivation Base for Nonmetal Composites and Functional Materials, Southwest University of Science and Technology, Sichuan, Mianyang 621010, China
[c] Max Planck Institute for Solid State Research, Heisenbergstrasse 1, 70569 Stuttgart, Germany

HIGHLIGHTS

- A novel safety strategy to avoid overcharging, i.e. solid-state anti-overcharge additive, is proposed.
- The strategy can provide a high-potential and a long-period of anti-overcharge performance.
- The effectiveness of the solid-state anti-overcharge additives is confirmed in $LiCoO_2$/C and $LiMn_2O_4$/C full cells.

ARTICLE INFO

Article history:
Received 9 December 2013
Received in revised form
14 April 2014
Accepted 16 April 2014
Available online 26 April 2014

Keywords:
Redox shuttle
Electrode
Copper oxide
Safety
Lithium battery

ABSTRACT

Overcharge safety is the most crucial problem facing especially large-sized lithium-ion batteries (LIBs) packs owing to the inevitable inhomogeneity of charge-state for each cell. We propose a fresh safety strategy to avoid overcharging, i.e. the use of a solid-state anti-overcharge additive to perform an intrinsic overcharge protection. The mechanism is triggered from a solid-state composite cathode obtained by typically mixing a pre-selected transition-metal oxide with a certain cathodes thus constituting a composite cathode. The effectiveness of this strategy is demonstrated with an example of $LiCoO_2$/CuO (95:5 by weight) composite, which exhibits high-potential (up to 5 V vs. Li^+/Li) and long-period (month-level) anti-overcharge performance. It is found that the additive does not hurt the electrochemical cycling performance under normal operational conditions. This novel safety strategy is simple and flexible, which may open a new window to develop safer LIBs systems.

1. Introduction

For large-scale applications of lithium-ion batteries (LIBs) in the situations like solar or wind energy plants or grid storage, safety will become major criterion for the general acceptance of this electrochemical technology [1–6]. Overcharge is the most popular and dangerous problem because it occurs particularly in large-sized LIBs systems with multiple cells owing to the inevitable inhomogeneity of charge-state of individual component cells [7–11]. In the galvanostatic mode, overcharge leads to unwanted high-voltages in which truly serious consequences root, including thermal runaway [8], gas generation [9], short-circuits [10] and ultimately fire or explosion [11]. Therefore, the control of voltage-runaway is key to overcome overcharge hazards. As an external protection, electronic-circuit is commonly used but not inherently reliable owing to occasional function-failure thus leading to more serious hazards [7]. Hence, an intrinsic mechanism should be developed to achieve more reliable overcharge protection. The currently established solution is to use liquid electrolyte additives, which function through reversible oxidation/reduction starting at a defined voltage slightly higher than the end-of-charge voltage to consume excess charge [7,12–15]. However, such additives suited for higher-voltage cathode materials (e.g. $LiNi_{0.5}Mn_{1.5}O_4$ (4.7 V) [16], $xLi_2MnO_3 \cdot (1-x)LiMO_2$ (above 4.6 V) [17]) are very rare, and

* Corresponding author. Tel.: +86 551 63606971; fax: +86551 63601592.
** Corresponding author. CAS Key Laboratory of Materials for Energy Conversion, Department of Materials Science and Engineering & Collaborative Innovation Center of Suzhou Nano Science and Technology, University of Science and Technology of China, Anhui Hefei 230026, China.
E-mail addresses: cchchen@ustc.edu.cn (C.-H. Chen), yanyumse@ustc.edu.cn (Y. Yu).

http://dx.doi.org/10.1016/j.jpowsour.2014.04.077
0378-7753/

subject to numerous severe limitations, including cost, electrochemical and chemical stability, compatibility with the battery components, and especially definite solubility requirement. These shortcomings significantly restrict the feasibility of this development.

Herein, we propose and confirm a novel safety strategy to avoid overcharging, i.e. solid-state anti-overcharge additives, an intrinsic overcharge protection mechanism triggered from solid-state composite cathodes. These composite cathodes provide an appropriately high triggering-potential (up to 5 V vs. Li^+/Li) and a long-period (month-level) of anti-overcharge performance. To our best knowledge, this is the first time that such a concept of cathodes providing intrinsic overcharge protection with a good performance has been reported. In this study, the $LiCoO_2$/CuO composite is used as an example to demonstrate the fundamental mechanism.

2. Experimental

2.1. Materials and chemicals

$LiCoO_2$ (Huatian Co., Ltd, China), $LiMn_2O_4$ (Jinhe Co., Ltd, China) and CuO (Sinopharm Co., Ltd, China) were used as raw materials. To obtain the $LiCoO_2$/CuO composite materials, the suspension containing dispersed $LiCoO_2$ and CuO powder in alcohol was fully stirred and dried to evaporate solvent. For $LiCoO_2$/CuO materials, there were four samples of different CuO contents: 0%, 5%, 30% and 100% (pure CuO). In addition, $LiMn_2O_4$/CuO (5%CuO) samples were obtained through the same solution mixing method. The above composite materials were all used as cathode (positive) materials. The cathode electrode laminates were formed by casting a mixture of $LiCoO_2$/CuO (or $LiMn_2O_4$/CuO), acetylene black and poly(-vinylindene fluoride) (PVDF) (mass ratio of 84:8:8) onto Al foil. They were dried and then punched into 14 mm diameter discs. The electrode active-substance loading was 12–15 mg (around 9.8 mg cm^{-2}) for each electrode disc. Lithium foil or graphite electrode was used as the anode (negative) electrode. The graphite electrode was formed by casting a mixture of graphite and PVDF (mass ratio of 92:8) onto Cu foil then punched it into 14 mm diameter discs. Battery-grade electrolyte (Guotai-Huarong, 1M $LiPF_6$ in ethylene carbonate/diethyl carbonate (EC/DEC, 1:1 by mass)) and polypropylene separator film (Celgard) were used as received.

2.2. Batteries fabrication and characterization

Two kinds of cells were assembled in an argon-filled glove box (MBraun Labmaster 130) with 1 ppm H_2O and 1 ppm O_2 content. Electrochemical performance tests were carried out using CR2032 coin-type cells. The amount of electrolyte in each coin-type cell is generally around 0.09 mL unless otherwise noted. To monitor the gas generation, pressure measurements were performed using a pressure-container cell setup (MTI Inc., Hefei) equipped with a pressure gauge. In each pressure-container cell, the same cathode and anode discs as coin cells were used, but the amount of electrolyte is required at around 3 mL. The phase compositions and crystal structures were characterized by X-ray diffraction (XRD) (Rigaku TTR-III, Cu Kα radiation). Surface elemental composition analyses were determined by energy-dispersive X-ray spectroscopy (EDS) based on scanning electron microscopy (SEM, JEOL-6390 LA). The content of Cu element in electrolyte was detected using inductive coupled plasma-atomic emission spectrometry (ICP-AES, Optima 7300 DV, Perkin Elmer Corporation, USA). Electrochemical measurements were performed using a Battery Testing System (BTS-3008W, Neware, Shenzhen). The internal DC resistance was measured with current interruption technique. A resistance is determined based on a measurement of $\Delta V/\Delta I$ between a base current and a high current step. This was carried out by cutting off the current (zero current) for 1 min before charging process in each cycle, and collecting the changes of voltage (ΔV) and current (ΔI) before and after this interruption. Thus, the DC resistance are calculated as $R_{dc} = \Delta V/\Delta I$. All cells were overcharged with constant current (CC) mode.

3. Results and discussion

3.1. Effect of voltage-control on $LiCoO_2$/CuO composite cathode

The characteristic features leading to this study are revealed from the first charge voltage profile of a bare CuO(Al foil)/Li cell (Fig. 1a), exhibiting a short 5 V interval, followed by a drastic voltage-drop and a long-time low-voltage plateau. For such a voltage curve, Cu^{2+} ions are released into the electrolyte and then reduced into Cu^+ to establish an important durable Cu^{2+}/Cu^+ redox shuttle, which will be detailed later. As controlling voltage-runaway is key in the context of overcharge protection, such a behavior is exciting. Indeed, the usefulness of CuO as an additive is confirmed by the overcharge voltage profile of a ($LiCoO_2$ + 5%CuO)/Li cell, revealing similar features including voltage-drop and long-time low-voltage plateau (Fig. 1b). For comparison, an overcharged $LiCoO_2$/Li cell initially displays an identical profile before it

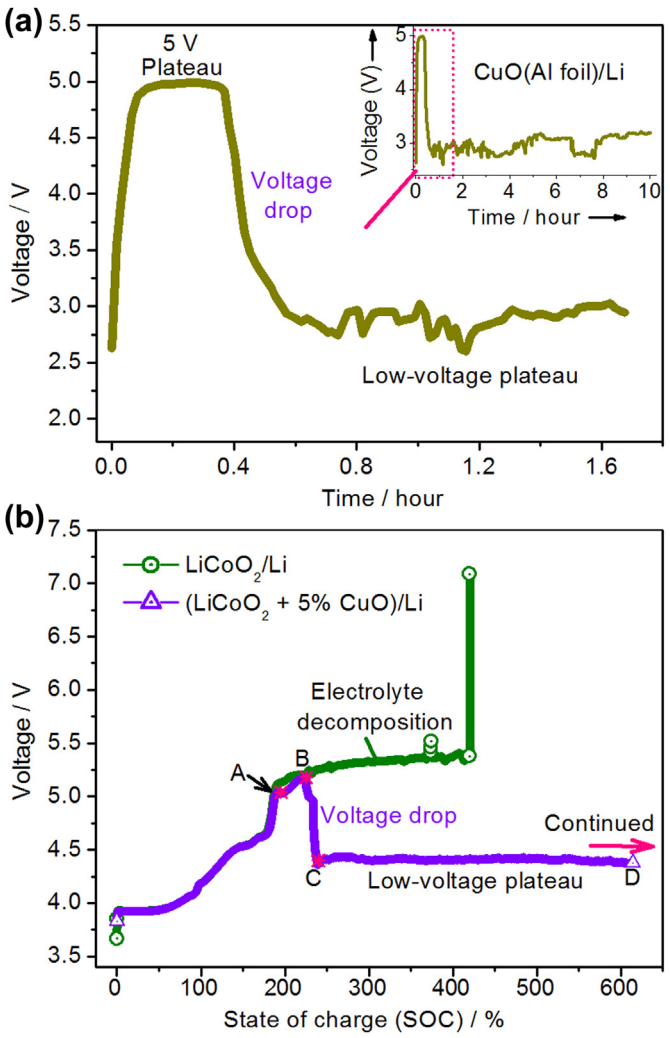

Fig. 1. Overcharge voltage profiles: a) CuO(Al foil)/Li coin cell (0.3 mA current). b) $LiCoO_2$/Li and ($LiCoO_2$ + 5%CuO)/Li coin cell (C/8 rate).

exceeds 5 V, but reaches a high-voltage plateau (5.2–5.4 V) which develops into an abrupt voltage-jump to 7 V (about 400% state-of-charge (SOC)) usually with further drastic consequences. The high-voltage plateau indicates irreversible decompositions of electrolyte and cathode [18]. Such damages are obviously inhibited in the ($LiCoO_2$ + 5%CuO)/Li cell because the long-time low-voltage plateau is far lower than the decomposition potential of the electrolyte [3]. Obviously, the $LiCoO_2$/CuO composite plays a highly beneficial role in controlling voltage-runaway during overcharge. It should be mentioned that the "5%CuO" is roughly the minimum CuO content that shows the efficient anti-overcharge effect without decreasing too much the specific capacity of the overall electrode laminate.

3.2. Effect of anti-overcharge on $LiCoO_2$/CuO composite cathode

To obtain a more detailed insight into the anti-overcharge effect of the $LiCoO_2$/CuO composite cathode, we conduct three in-depth investigations as below.

Firstly, we demonstrate that within the normal voltage window (2.8–4.2 V), a ($LiCoO_2$ + 5%CuO)/Li cell operates with nearly identical performance as a $LiCoO_2$/Li cell, with a coulombic efficiency of around 99% and a capacity retention of 94% at the 50th cycle (Fig. 2a). The results suggest stability and compatibility of the cathode component CuO against $LiCoO_2$ cathodes and no significant evidence of negative effects on the electrochemical performance is observed.

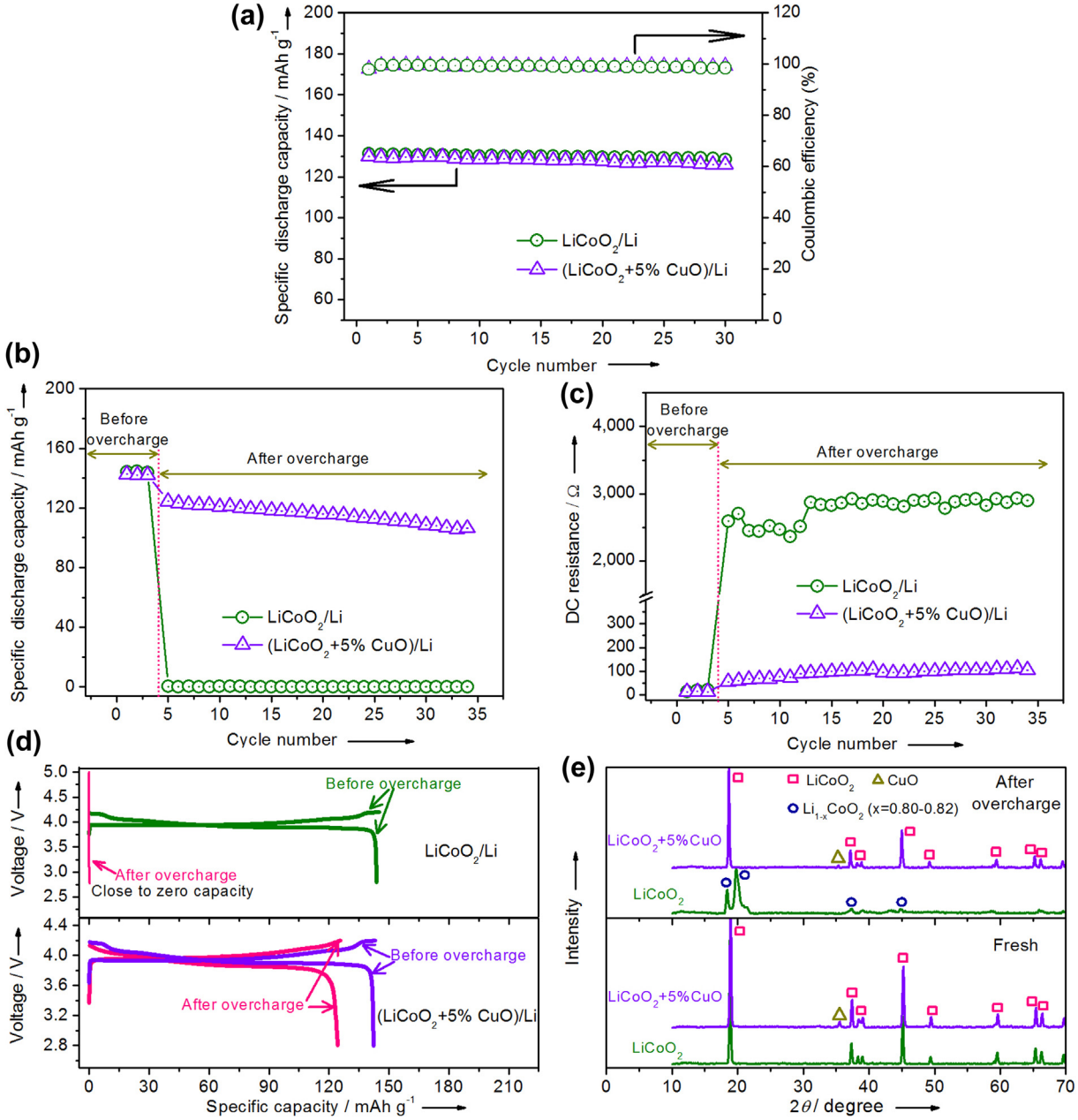

Fig. 2. Electrochemical characterization comparisons of ($LiCoO_2$ + 5%CuO)/Li and $LiCoO_2$/Li coin cells: normal cycling capacity and coulombic efficiency comparisons (2.8–4.2 V, C/2 current) (a), cycling capacity (b), direct-current (DC) resistance (c), and typical charge/discharge voltage curves (d) before and after the overcharge. The cells are both firstly charged/discharged for 3 cycles (2.8–4.2 V, C/5) and then overcharged for around 40 h (C/8), followed by a continued normal cycling (2.8–4.2 V, C/5). The XRD patterns of cathodes (stripped from Al foil) of the cells in (b) are also given in (e). "Fresh" (lower panel) represents the cathode discs before the cell assembling. Upper panel represents the cathode discs at the end-of-discharge state in 5th cycle after overcharge for the cells in (b).

Secondly, we investigate the difference after overcharge in the discharge capacity and in the direct-current (DC) resistance between the two cells under comparison (Fig. 2b and c). Before overcharge, they display comparable discharge capacities (140 mA h g^{-1}) and DC resistances (15–20 Ω). After overcharge, the ($LiCoO_2$ + 5% CuO)/Li cell still maintains considerable capacity (125 mA h g^{-1}), perfect columbic efficiency (99%), stable cyclability and low DC resistance (50–100 Ω). In contrast, the $LiCoO_2$/Li cell after overcharge shows almost no capacity (0.2 mA h g^{-1}) and quite high DC resistance (2500–2900 Ω) owing to serious irreversible damages to the electrode material or electrolyte. In addition, the typical voltage profile of the ($LiCoO_2$ + 5%CuO)/Li cell is maintained after overcharge, in sharp contrast to the overcharged $LiCoO_2$/Li cell (Fig. 2d).

XRD measurements (Fig. 2e) on cathodes end-of-discharge state (normal 5th cycle after overcharge) reveal that in case of the cathode of the ($LiCoO_2$ + 5%CuO)/Li cell, the initial $LiCoO_2$ phase is recovered. This is not the case for the cathode of the $LiCoO_2$/Li cell here, and only a delithiated composition $Li_{1-x}CoO_2$ (x = 0.80–0.82) is obtained here [19], which is consistent with the above capacity results. Hence, the $LiCoO_2$/CuO composite can definitely avoid irreversible damages during overcharge and maintain reversible charge/discharge performance after overcharge.

Thirdly, in order to explore the mechanism of the anti-overcharge effect, we perform pressure measurements of a possible gas generation from electrolyte decomposition during overcharge (Fig. 3). Obviously, the ($LiCoO_2$ + 30%CuO)/Li cell as well as the $LiCoO_2$/Li cell generates negligibly low pressures (1–2 kPa) in the initial period. However, beyond 200% SOC, the pressure of the $LiCoO_2$/Li cell starts to rise and then rapidly reaches a very high value (22.3 kPa), while the pressure of ($LiCoO_2$ + 30%CuO)/Li cell changes very slowly to a value (5 kPa) that is not exceeded on further charging (Fig. 3a). This pressure experiment clearly implies that during overcharge, the $LiCoO_2$/Li cell suffers from serious electrolyte decomposition leading to significant gas generation, while the electrolyte in the ($LiCoO_2$ + 30%CuO)/Li cell remains stable as decomposition and gas generation are largely inhibited owing to avoidance of voltage-runaway. Note that here, for this type of pressure-container cell, ($LiCoO_2$ + 30%CuO)/Li is used instead of ($LiCoO_2$ + 5%CuO)/Li because no obvious voltage-controlling feature is observed in the ($LiCoO_2$ + 5%CuO)/Li cell owing to the low function concentration resulting from more electrolytes required in each pressure-container cell set (3 mL) than coin cell (0.09 mL) (detailed later). In addition, after the overcharge pressure measurements, the electrolyte collected from the disassembled $LiCoO_2$/Li cell appears yellow (possible phosphorous products) while the electrolyte from the ($LiCoO_2$ + 30%CuO)/Li cell has maintained its initial transparency as fresh (Fig. 3b).

3.3. Analysis of the anti-overcharge mechanism

For a more comprehensive understanding, we need to explore the nature of the short 5 V plateau, the voltage-drop and the steady-state low-voltage plateau. The two independent plateaus actually suggest two different processes. The analysis of the CuO(Al foil)/Li cell after overcharge shows that the only cathode phase is CuO (Fig. 4a), and at the anode Li plate (Fig. 4b and c) we observe no other elements except C, O, F, P together with Li consisting the Solid Electrolyte Interface (SEI) film. But we detect Cu in the electrolyte, implying that CuO partially decomposed at 5 V.

For the short plateau at 5 V (Figs. 1a, b and 3a), the plausible reaction mechanism can be formulated (similar to the oxidation of Li_2O_2 in Li–O_2 battery [20]) as

$$\text{Cathode}: \quad CuO \xrightarrow{\text{Charge}} Cu^{2+} + 0.5O_2\uparrow + 2e^- \tag{1}$$

$$\text{Anode}: \quad 2Li^+ + 2e^- \xrightarrow{\text{Charge}} 2Li \tag{2}$$

The calculated standard potential for reaction (1) (vs. Li/Li^+ in aqueous solution) is around 4 V. If we take into account that oxygen pressure and Cu^{2+} concentration are far from standard conditions, that we refer to a different solvent and over-voltage must be included, the observed 5 V plateau can be affiliated with the above reaction. The generated Cu^{2+} ions will be dissolved in the electrolyte, diffuse to the anode, and then trigger a new reaction (Cu^{2+} reduction).

As far as the voltage-drop (BC period in Fig. 1b) and the subsequent low-voltage plateau (CD period in Fig. 1b) is concerned, the variation of the electrolyte volume (with electrode distance being kept constant, ~0.5 mm) is very revealing (Fig. 5). The characteristic results are that the steady-state low-voltage strongly depends on the electrolyte volume, while the width of the high-voltage plateau does not vary much. The time window (Fig. 1b) from A to B (10^3 s level) well conforms with the time required for Cu^{2+} to travel from cathode to anode (if a typical diffusion coefficient of 10^{-6}~10^{-7} cm^2 s^{-1} is taken). At the anode side Cu^{2+} will be reduced but we did not observe Cu-plating probably because the SEI impedes Cu-nucleation [21,22].

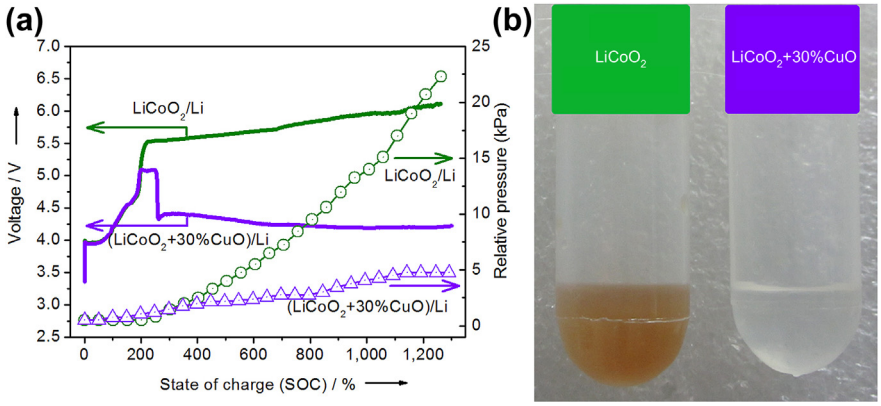

Fig. 3. Pressure measurement to evaluate gas generation during overcharge and photographs of the electrolytes after overcharge for the ($LiCoO_2$ + 30%CuO)/Li and $LiCoO_2$/Li pressure-container cells. Note that here, more electrolytes (3 mL) are required in each pressure-container cell set than general coin cell (0.09 mL), thus, ($LiCoO_2$ + 30%CuO)/Li but not ($LiCoO_2$ + 5%CuO)/Li is utilized to maintain an efficient function concentration of Cu-ions injected into electrolyte. a) Overcharge pressure and voltage profile during overcharge (0.8 mA). b) Photographs of the electrolytes collected from the disassembled cells after the overcharge in (a).

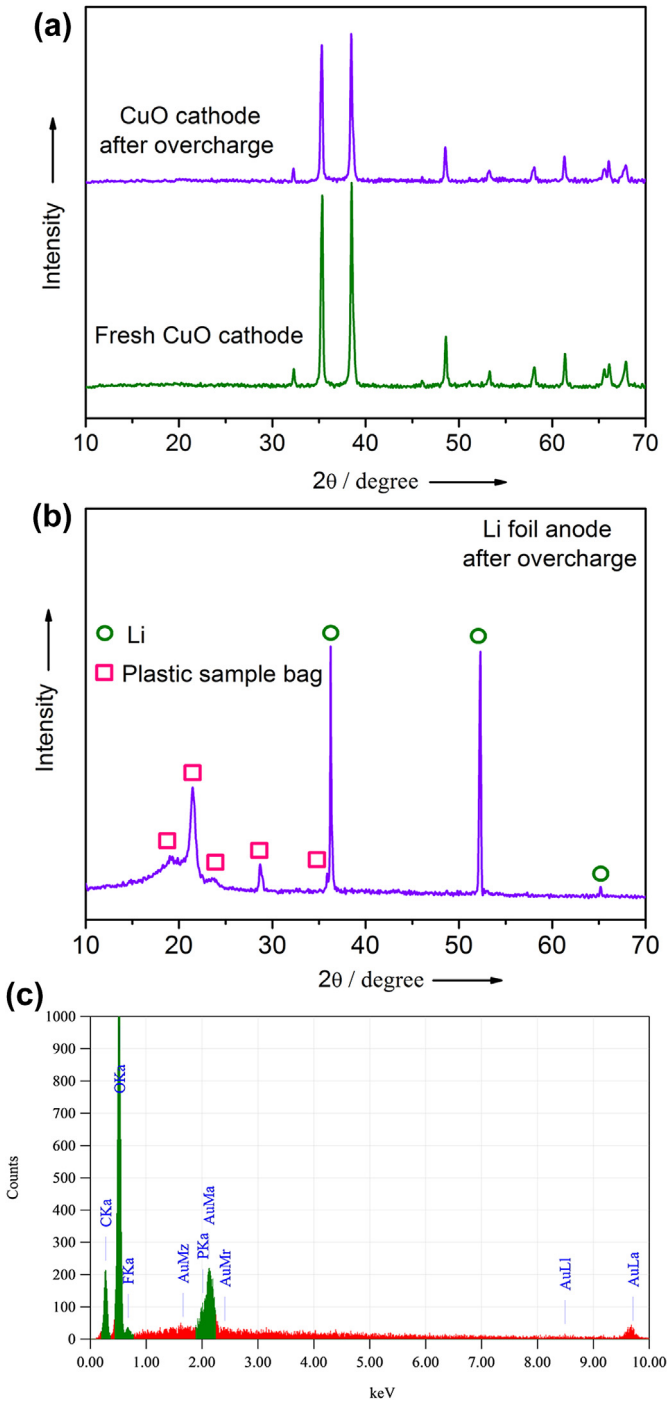

Fig. 4. Characterization of CuO(Al foil)/Li coin cell after overcharge. The cell is overcharged for 10 h at 0.3 mA (see Fig. 1a). a) XRD patterns comparison of cathode discs (stripped from Al foil) between the overcharged (upper panel) and a fresh cathode electrode (lower panel). The fresh electrode represents the cathode disc before the cell assembling. b) XRD patterns of anode Li foil after overcharge. The Li foil is sealed in plastic sample-bag to prevent oxidation. c) EDS analyses to Li foil surface after overcharge. C, O, F and P elements are clearly detected but Cu element (8 keV) is not detected. In addition, ICP-AES analysis to the collected DMC soak solution shows that a few of Cu element is detected in overcharged electrolyte of the cell.

Hence, we conclude that Cu^{2+} is reduced into Cu^{+} at the anode side. Consequently, the Cu^{2+}/Cu^{+} shuttle reaction can be considered to be a reasonable explanation for such a long-time low-voltage plateau (even 10,000% SOC and 40,000% SOC in Fig. 6), establishing an efficient internal safety-passage consuming current.

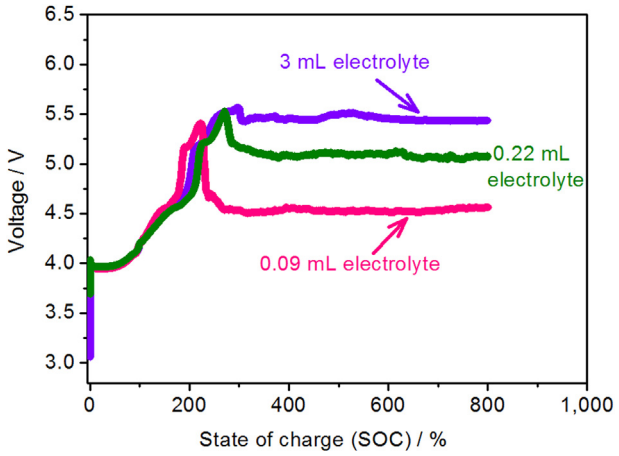

Fig. 5. Overcharge voltage profile for ($LiCoO_2$ + 5%CuO)/Li cell (around C/2 rate) with different amount of electrolytes: 0.09 mL and 0.22 mL (coin cells) and 3 mL (pressure-container cell).

At the cathode side we now refer, instead of Eq. (1), to the redox process $Cu^{+} \leftrightarrow Cu^{2+} + e^{-}$, while at the anode side, a mixed potential develops characterized by the two competing processes $Li^{+} + e^{-} \leftrightarrow Li$ (cf. Eq. (2)) and $Cu^{2+} + e^{-} \leftrightarrow Cu^{+}$. As a consequence we refer to two parallel cell reactions, of which the Cu^{2+}/Cu^{+} shuttle reaction contributes with a standard potential of 0 V [12,15]. This is supported by the following three observations (See Fig. 5): (i) The value of the low-voltage plateau is distinctly reduced; (ii) The value is the smaller with the higher Cu-ion concentration (smaller electrolyte volume); (iii) The low-voltage stays constant during charging owing to the constant Cu-ion concentration fixed by high-voltage prehistory (amount of CuO decomposed). These results clearly confirm that the low-voltage plateau roots in the electrolyte and is Cu-ion concentration dependent, typical characteristic of a redox shuttle [12,15].

Additionally, the Cu-ions will be distinctly solvated owing to the interaction of Cu^{n+}-ions with the highly polar C=O groups (empty π^{*}-antibonding orbital) of aprotic EC/DEC electrolyte solvents [23,24], and soft-base EC/DEC solvents can easily solvate the soft-acid Cu^{+} or Cu^{2+} cations according to the Hard and Soft Acids and Bases (HSAB) theory [25]. As a result, Cu^{2+} or Cu^{+} is expected to form rather stable complexes in aprotic EC/DEC solvents, enhancing the difficulty of Cu-formation here.

These findings lead to the following consistent scenario. On overcharge CuO starts decomposing (Eq. (1)) thus preventing electrolyte decomposition. The injected Cu^{2+} ions travel towards the anode where they are reduced. Subsequently, the Cu^{2+}/Cu^{+} redox pair acts as a shuttle maintaining a stable and safe low-voltage. In this way not only serious hazards are avoided but also the cell-functions remain largely intact.

3.4. The application of the solid-state anti-overcharge additive in full cells

As far as applied electrochemistry science is concerned, the application in full cells of this strategy makes the protection mechanism particularly relevant for Li-ion batteries revealing potential wide extending space. First, the mechanism featured by the voltage-drop and low-voltage plateau can be reasonably extended to practical ($LiCoO_2$ + 5%CuO)/graphite cells (Fig. 6a). Also, no significant negative effect to the normal full-cell performance is observed, when CuO is added into $LiCoO_2$ cathode (Fig. 6b). Second, the mechanism and its effect on the full cells can also be extended

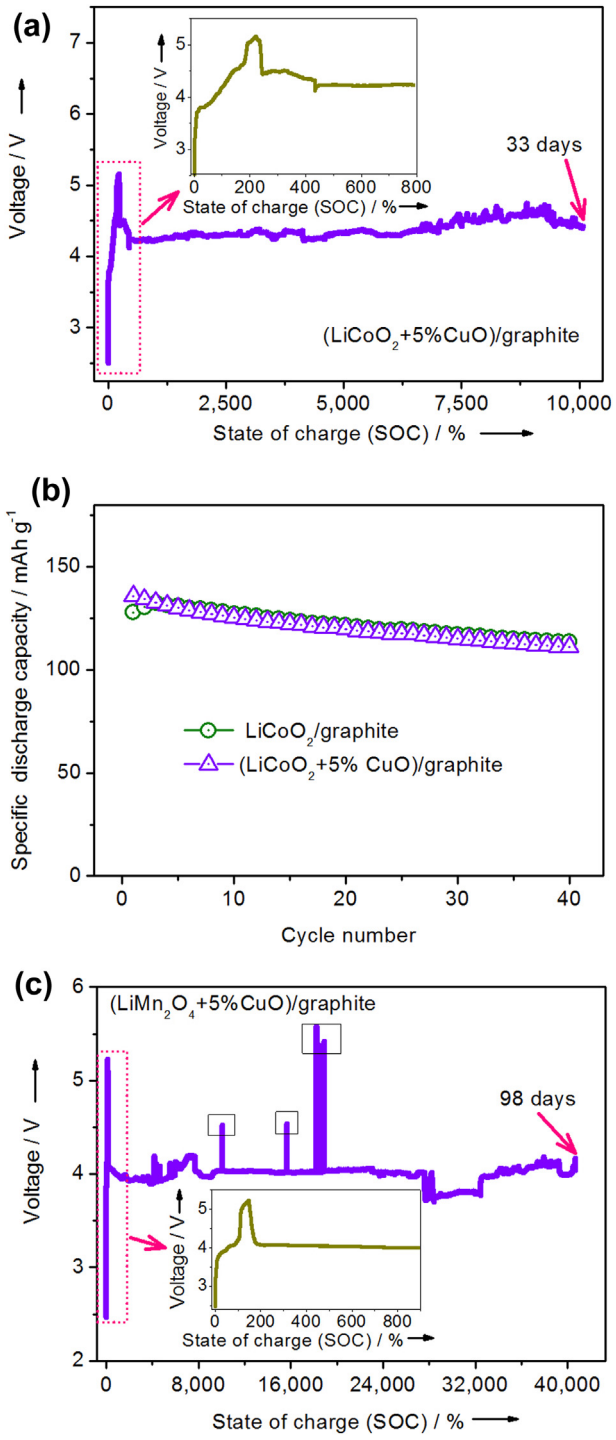

Fig. 6. Extending of the novel anti-overcharge strategy in full cells. a) Overcharge voltage profile for a ($LiCoO_2$ + 5%CuO)/graphite coin cell (C/8). b) Normal cycling comparison between $LiCoO_2$/graphite and ($LiCoO_2$ + 5%CuO)/graphite coin cells (2.8–4.2 V, C/2). c) Overcharge voltage profile for a ($LiMn_2O_4$ + 5%CuO)/graphite coin cell (C/6). Inset in (a) and (c): Enlargement of dotted area. Some abrupt voltage-jump points in (c) (box marked) are possibly due to power interruption.

to the other popular cathode materials working below 5 V ($LiMn_2O_4$, $LiFePO_4$, etc). As an example, Fig. 6c demonstrates the characteristic voltage-controlling effect also for overcharged ($LiMn_2O_4$ + 5%CuO)/graphite cells. It is important to note that overcharges corresponding to more than 100 times (10,000% SOC, C/8, 33 days) and 400 times (40,000% SOC, C/6, 98 days) of the cell-nominal-capacity can still be digested in the ($LiCoO_2$ + 5%CuO)/graphite and ($LiMn_2O_4$ + 5%CuO)/graphite cell, respectively, even during a long-time (month-level) overcharge.

In addition to CuO, our ongoing work shows that some other transition-metal oxides display similar voltage-controlling features and can also provide protection in other voltage ranges, offering far-reaching possibilities for individually selecting appropriate solid-state additive for a specific cell system.

4. Conclusions

We propose and confirm a fresh safety strategy, i.e. solid-state anti-overcharge additives, for high performance LIBs by using composite cathodes with built-in redox overcharge protection. This strategy may open a new window to develop safer LIBs systems.

Acknowledgments

The authors acknowledge the National Natural Science Foundation of China (Nos. 20971117, 10979049, 21171015, 21373195 and J1030412) and the Open Project of State Key Laboratory Cultivation Base for Nonmetal Composites and Functional Materials (No. 11zxfk26). This work is also financially supported from Sofja Kovalevskaja Award from Alexander von Humboldt Foundation, the "1000 plan" from Chinese Government, the Fundamental Research Funds for the Central Universities (WK2060140014, WK2060140016) and Program for New Century Excellent Talents in University.

References

[1] M. Armand, J.M. Tarascon, Nature 451 (2008) 652–657.
[2] B. Dunn, H. Kamath, J.M. Tarascon, Science 334 (2011) 928–935.
[3] J.B. Goodenough, Y. Kim, Chem. Mater. 22 (2009) 587–603.
[4] N.S. Choi, Z. Chen, S.A. Freunberger, X. Ji, Y.K. Sun, K. Amine, G. Yushin, L.F. Nazar, J. Cho, P.G. Bruce, Angew. Chem. Int. Ed. 51 (2012) 9994–10024.
[5] P.G. Bruce, B. Scrosati, J.M. Tarascon, Angew. Chem. Int. Ed. 47 (2008) 2930–2946.
[6] J.W. Wen, Y. Yu, C.H. Chen, Mater. Express 2 (2012) 197–212.
[7] Z. Chen, Y. Qin, K. Amine, Electrochim. Acta 54 (2009) 5605–5613.
[8] Y. Saito, K. Takano, A. Negishi, J. Power Sources 97–98 (2001) 693–696.
[9] T. Ohsaki, T. Kishi, T. Kuboki, N. Takami, N. Shimura, Y. Sato, M. Sekino, A. Satoh, J. Power Sources 146 (2005) 97–100.
[10] R. Bhattacharyya, B. Key, H. Chen, A.S. Best, A.F. Hollenkamp, C.P. Grey, Nat. Mater. 9 (2010) 504–510.
[11] P. Ribiere, S. Grugeon, M. Morcrette, S. Boyanov, S. Laruelle, G. Marlair, Energy Environ. Sci. 5 (2012) 5271–5280.
[12] K. Xu, Chem. Rev. 104 (2004) 4303–4417.
[13] S.S. Zhang, J. Power Sources 162 (2006) 1379–1394.
[14] J.R. Dahn, J. Jiang, L.M. Moshurchak, M.D. Fleischauer, C. Buhrmester, L.J. Krause, J. Electrochem. Soc. 152 (2005) A1283–A1289.
[15] S.R. Narayanan, S. Surampudi, A.I. Attia, C.P. Bankston, J. Electrochem. Soc. 138 (1991) 2224–2229.
[16] J.H. Kim, S.T. Myung, C.S. Yoon, S.G. Kang, Y.K. Sun, Chem. Mater. 16 (2004) 906–914.
[17] M.M. Thackeray, S.-H. Kang, C.S. Johnson, J.T. Vaughey, R. Benedek, S.A. Hackney, J. Mater. Chem. 17 (2007) 3112–3125.
[18] G. Girish Kumar, W.H. Bailey, B.K. Peterson, W.J. Casteel, J. Electrochem. Soc. 158 (2011) A146–A153.
[19] X. Sun, X.Q. Yang, J. McBreen, Y. Gao, M.V. Yakovleva, X.K. Xing, M.L. Daroux, J. Power Sources 97–98 (2001) 274–276.
[20] T. Ogasawara, A. Débart, M. Holzapfel, P. Novák, P.G. Bruce, J. Am. Chem. Soc. 128 (2006) 1390–1393.
[21] A. Kominato, E. Yasukawa, N. Sato, T. Ijuuin, H. Asahina, S. Mori, J. Power Sources 68 (1997) 471–475.
[22] D. Aurbach, I. Weissman, A. Schechter, H. Cohen, Langmuir 12 (1996) 3991–4007.
[23] K. Izutsu, Electrochemistry in Nonaqueous Solutions, Wiley-VCH Verlag GmbH & Co. KGaA, Weinheim, 2003.
[24] L. Yu, H. Liu, Y. Wang, N. Kuwata, M. Osawa, J. Kawamura, S. Ye, Angew. Chem. Int. Ed. 52 (2013) 5753–5756.
[25] R.G. Pearson, J. Am. Chem. Soc. 85 (1963) 3533–3539.